ISSN: 2414-1895 DOI: 10.6919/ICJE.202104_7(4).0015

Mechanical Fault Diagnosis of High Voltage Circuit Breaker Based on Acoustic Vibration and IFPA-SVM

Xiaoxue Chen*, Hejin Yuan[a], Weihua Niu[b] and Kebin Cui[c]

Department of Computer, North China Electric Power University, Baoding 071003, China.

*1175133619@qq.com, [a]651344234@qq.com, [b]10356274@qq.com, [c]ncepuckb@163.com

Abstract

In order to classify the faults of high voltage circuit breakers more efficiently, a fault diagnosis method based on the combination of acoustic vibration and support vector machine (SVM) optimized by improved flower pollination algorithm (IFPA) is proposed. Firstly, ensemble empirical mode decomposition (EEMD) and EEMD - improved wavelet threshold function are used to denoise the vibration and sound signals of circuit breakers respectively, and then the energy entropy of the vibration and sound signals is extracted. Finally, the feature fusion of acoustic and vibration signals is input into the support vector machine(SVM) model optimized by IFPA to realize the diagnosis among different fault categories. The experiment on high voltage circuit breaker proves the effectiveness of the new method.

Keywords

Combination of Sound and Vibration; Ensemble Empirical Mode Decomposition; Improved Wavelet Threshold Function; Improved Flower Pollination Algorithm; Fault Diagnosis.

1. Introduction

The operation of high voltage circuit breaker is related to the stability and safety of the power grid, and mechanical failure is the main fault of the high voltage circuit breaker. Therefore, it is of practical engineering value to study the mechanical fault diagnosis of high voltage circuit breaker.

In recent years, most fault diagnosis methods are to extract useful features from signals and input feature vectors into classifiers to judge the state of equipment. Among them, Jia Jin Qi et al. [1] divided the vibration signal of circuit breaker in time domain, extracted 16 features as feature vectors, and input them into classifier for classification. Linhua Luo et al. [2] used the improved MFCC algorithm to extract the characteristic parameters of the discharge audio signal to realize the circuit breaker fault diagnosis. Hengzhen Li et al. [3] used wavelet de-noising method to denoise the current signal of circuit breaker, and then extracted the current characteristics and input it into SVM for fault diagnosis. Yu Yao et al. [4] combined fractal technology with probabilistic neural network and proposed a new research method of circuit breaker fault diagnosis model. Shi Liu et al. [5] proposed a circuit breaker fault diagnosis method based on PSO-BP neural network, which has higher accuracy than the traditional BP neural network model.

The above methods have made a lot of improvements in the fault diagnosis model, but there are still some shortcomings: a single signal description is one-sided, some faults can not be distinguished. the preprocessing method does not analyze according to the specific characteristics of the signal. the fault diagnosis model needs more samples, and the parameter optimization algorithm is easy to fall into the minimum value.

ISSN: 2414-1895 DOI: 10.6919/ICJE.202104_7(4).0015

In order to solve the above problems, this paper proposes a mechanical fault diagnosis method based on the combination of acoustic and vibration. Firstly, EEMD and EEMD wavelet threshold are used to denoise the vibration signal and sound signal, and then the feature entropy of the signal is extracted respectively. Finally, feature fusion is used as input vector and input to IFPA optimized support vector machine for classification. The effectiveness of this method is verified by comparing with flower pollination algorithm(FPA), particle swarm optimization algorithm(PSO) and shuffled frog leaping algorithm(SFLA).

2. Signal preprocessing and feature extraction

2.1 Principle of EEMD

EEMD [6] is an adaptive time-frequency processing method suitable for nonlinear and non-stationary signals. Firstly, white noise is added to the signal, and then the mixed signal is decomposed into IMF of different time scales, as shown in formula (1). Then, the IMF component and residual are obtained by the full average operation of each component to eliminate the influence of white noise. It weakens the mode aliasing in empirical mode decomposition (EMD).

$$x(t) = \sum_{i=1}^{n} imf_i(t) + r_n(t) \tag{1}$$

2.2 Improved Wavelet threshold denoising.

Wavelet threshold de-noising firstly decomposes the signal by wavelet, then processes the wavelet coefficients by threshold function, and finally reconstructs the denoised signal. Among them, the classical wavelet threshold functions include hard threshold function and soft threshold function. The former has breakpoints, while the latter is prone to distortion. Based on the above shortcomings, an improved threshold function is proposed. The formula is as follows:

$$\omega_{j,k}^{'} = \begin{cases} sign(\omega_{j,k})(|\omega_{j,k}| - \frac{\lambda}{\sqrt{1+\ln N_j}^{a*(|\omega_{j,k}|-\lambda)}}) & |\omega_{j,k}| \geq \lambda \\ 0 & |\omega_{j,k}| < \lambda \end{cases} \tag{2}$$

In the formula, N_j is the length of wavelet coefficients of the j layer, and the trend of threshold function is adjusted by adjusting factor a $\in[0,+\infty)$. When a→0, the whole tends to soft threshold; when a→∞, the whole tends to hard threshold; when $\omega_{j,k}\to\lambda$, $\omega'_{j,k}\to 0$, which ensures the continuity of $\omega_{j,k}=\lambda$. In this paper, the layered threshold [7] is used to denoise the signal.

2.3 Signal denoising and feature extraction.

Firstly, the acoustic vibration signal is decomposed by EEMD to obtain a series of IMF components. Then the IMF component of the acoustic signal is denoised by improved wavelet threshold. Finally, the high-frequency component is reconstructed to obtain the denoised signal. Then the energy entropy [8] is extracted as the feature vector.

3. Parameter optimization of SVM model

3.1 SVM fault diagnosis model.

SVM is a classification model, which can be used for kernel function nonlinear classification. In this paper, radial basis function is used, including penalty parameter c and kernel function parameter g [9]. The accuracy of SVM classification depends on the parameters c and g to a great extent. In this paper, the idea of leapfrog [10] is introduced on the basis of FPA [11] to improve the local search ability of the algorithm. Combined with hybrid mutation strategy [12], the algorithm has mutation function. The algorithm steps are as follows.

Step 1: Initialize parameters and positions. The position of individuals is parameters c and g. the global optimal individuals are determined by calculating the classification accuracy(fitness).

Step 2: Within the number of iterations, follow step 4 to iteratively update all individuals.

ISSN: 2414-1895 DOI: 10.6919/ICJE.202104_7(4).0015

Step 3: Generate a random number rand1 on [0,1]. If rand1 is less than the conversion probability p, cross pollination will be carried out and the individual position will be updated according to formula (4) and formula (5); otherwise, self pollination will be carried out, that is, the position will be updated according to formula (6).

$$X_i^{t+1} = X_i^t + L(g^* - X_i^t) \tag{4}$$

In formula (4), *Xt+1 i* and *Xt i* are the solutions of generation *t*+1 and generation *t* respectively, g^* is the global optimal solution, *L* is the step size, and the formula is as follows:

$$L \sim \frac{\lambda\Gamma(\lambda)\, sin(\pi\lambda/2)}{\pi} \frac{1}{s^{1+\lambda}}, (s >> s_o > 0) \tag{5}$$

In formula (5), λ = 3/2, r(λ) is the standard gamma function and S is the moving step size.

$$x_i^{t+1} = x_i^t + \varepsilon(x_j^t - x_k^t) \tag{6}$$

In formula (6), ε is the constant of uniform distribution on [0,1], and *Xt j* and *Xt k* are different pollens of the same generation.

Step 4: After all individuals are updated once, local search is performed. The fitness values of all individuals were calculated and arranged in ascending order. According to formula (7), there were n individuals in each meme group. M^k is the *k*th meme group. The fitness value *gb* and its spatial position of the current optimal individual were recorded.

$$M^k = \{X_{k+m(t-1)}^t \in P | 1 \le l \le n\}, 1 \le k \le m \tag{7}$$

Step 5: Determine the *pb* and *pw* of the best and worst individuals in each meme group, update the best in the group according to formula (8) and formula (9), and update *pw* if the fitness value is better than the fitness of *pw*, otherwise, use formula (8) and formula (10) to update the global optimum, if the fitness value is better than the fitness of *pw*, update *pw*, otherwise, use formula (11) to update Cauchy Variation, PW was updated randomly.

$$pw' = pw + s, \| s \| \le s\max \tag{8}$$

$$s = rand * (pb - pw) \tag{9}$$

$$s = rand * (gb - pw) \tag{10}$$

$$pw' = pw + pw * Cauchy(0,1) \tag{11}$$

Step 6: Generate a random number rand2 on [0,1]. If rand2 is less than the variation factor *g*, Gaussian mutation is performed by using equation (12). If the fitness is better than that of *pb*, update *pb*, otherwise, discard the mutated solution. When all meme groups were updated, all individuals were mixed to form a new species group.

$$pb' = pb + pb * N(0,1) \tag{12}$$

Step 7: Recalculate the fitness value of the new species group and determine the current global optimal individual *gb*. If the fitness value of *gb* is better than that of the previous generation, the global optimal information will be updated.

Step 8: Judge whether the termination condition is satisfied, if so, exit the program, otherwise, calculate repeatedly until the optimal solution is found.

Convergence condition: When the global optimal value remains unchanged after several iterations or the total number of iterations is reached, the algorithm is terminated.

3.2 Test of algorithm performance.

The performance of the algorithm is tested by Griewank multimodal function of formula (13).

$$\frac{1}{400}\sum_{i=1}^{n} {x_i}^2 - \prod_{i=1}^{n} cos\frac{x_i}{\sqrt{i}} + 1 \tag{13}$$

IFPA is compared with PSO, FPA and SFLA, as shown in Fig. 1. Dimension: 20, number of iterations: 200, IFPA: n=4, m=5, p=0. 8, g=0. 1. PSO: NP=20. FPA: p=0. 8. SFLA: n=4, m=5.

ISSN: 2414-1895 DOI: 10.6919/ICJE.202104_7(4).0015

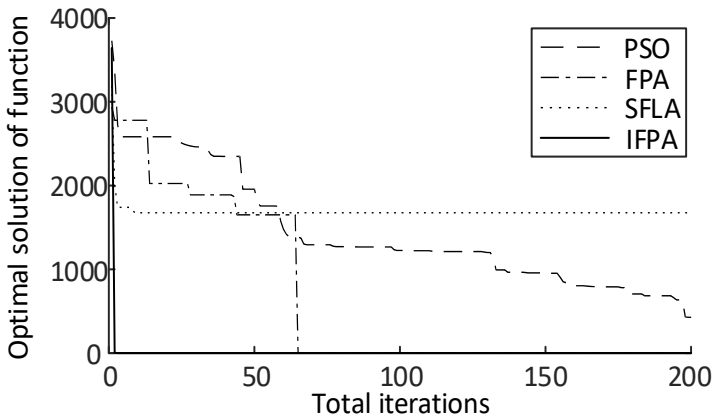

Fig. 1 Optimization results of PSO, FPA, SFLA and IFPA algorithms

Compared with PSO and SFLA, IFPA has stronger ability of high-dimensional function optimization. Compared with FPA, IFPA can converge to the optimal solution faster.

4. Experimental analysis

4.1 Data acquisition and fault diagnosis process.

In the experiment, Z65 vacuum circuit breaker was used to simulate four states: normal closing, pedestal loosening, refusing closing, connecting rod falling off between closing spring and opening spring. The four states were simulated for 20 times and 80 groups of data were obtained. The sampling frequency is 25.6khz/s, and the diagnosis process is shown in Figure 2.

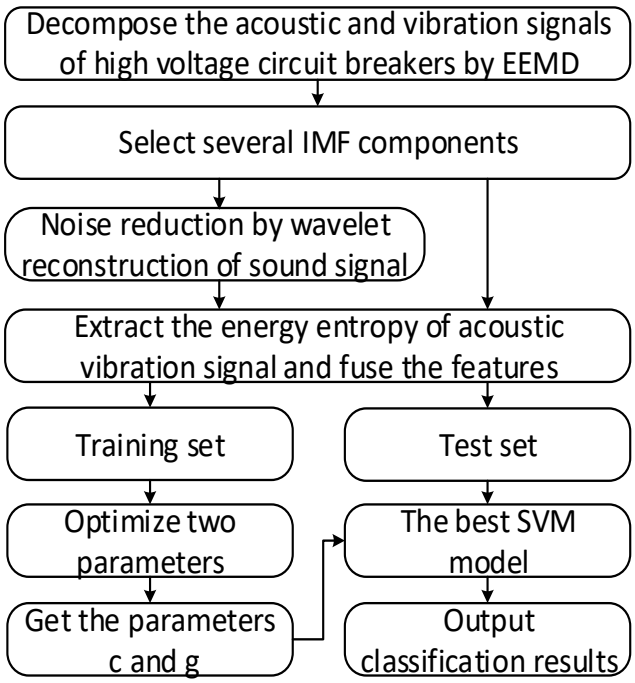

Fig. 2 Fault diagnosis flow chart of circuit breaker

4.2 Data preprocessing and feature extraction.

Due to the space limitation, this paper analyzes the signal by taking the failure of closing as an example, and its waveform is shown in Fig. 3.

ISSN: 2414-1895 DOI: 10.6919/ICJE.202104_7(4).0015

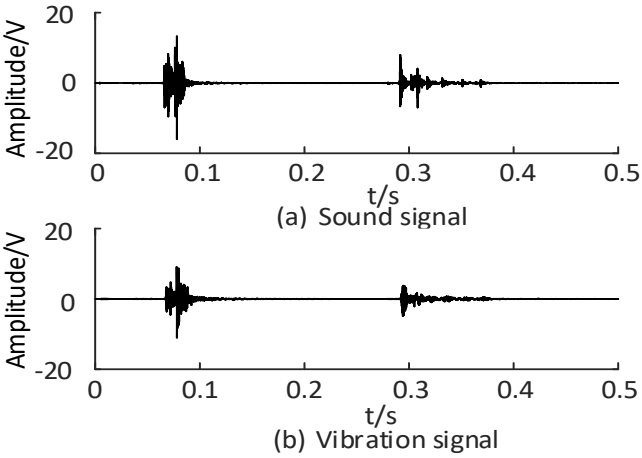

Fig. 3 Time domain diagram of sound and vibration signals of refuse to close fault

The amplitude of sound signal is large and its noise is obvious, so wavelet threshold denoising is only applied to IMF component of sound signal. Firstly, EEMD is used to decompose the acoustic vibration signal. Taking the sound signal as an example, it can be decomposed into 8 components and 1 margin. The decomposition diagram and the spectrum of each component are shown in Figure 4.

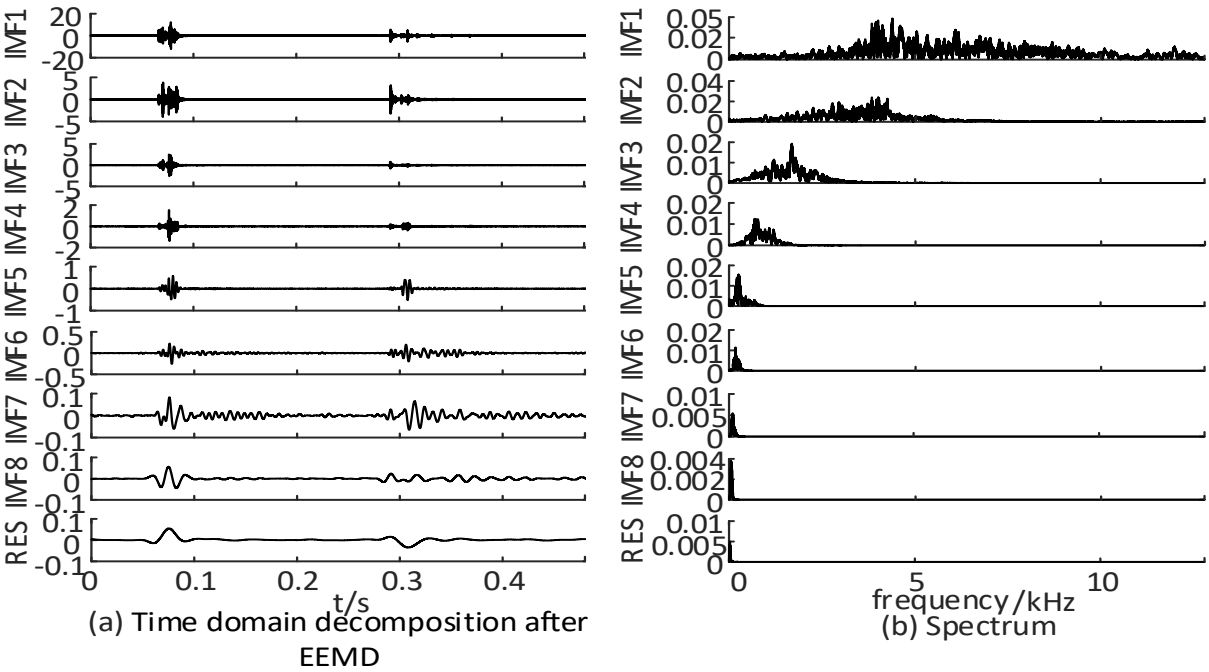

Fig. 4 EEMD decomposition and spectrum of sound signal

The wider the frequency band, the more noise it contains. The frequency band of the first five IMF components is relatively wide, so the first five IMF components are selected for noise reduction. Combined with the correlation coefficient, select the component to retain the effective information, as shown in Table 1.

Table 1. Correlation coefficient of each IMF component

	IMF1	IMF2	IMF3	IMF4	IMF5	IMF6	IMF7	IMF8
correlation coefficient	0. 901	0. 380	0. 114	0. 123	0. 100	0. 078	0. 022	0. 003

ISSN: 2414-1895 DOI: 10.6919/ICJE.202104_7(4).0015

If the correlation coefficient is greater than or equal to 0.1, it means that the component retains the effective information of the signal. Therefore, the first five order components are selected for reconstruction. Finally, the first five IMF components are reconstructed by combining spectrum and correlation coefficient. The reconstructed signal is shown in Figure 5.

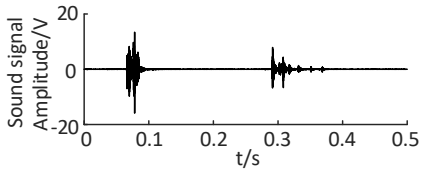

Fig. 5 Sound signal after noise reduction

In order to verify the denoising effect, the original signal is added to the noise with signal-to-noise ratio of 5dB. EEMD and its combined with three threshold functions are used to reduce noise respectively. The noise reduction effect is compared, as shown in Table 2.

Table 2. Signal to noise ratio of EEMD and its combination with three wavelet threshold functions

Evaluation criteria	EEMD	EEMD + hard	EEMD+ Soft	EEMD+ Improved
NSR/dB	5. 0417	7. 8580	7. 9553	8. 5812

The N_{SR} of EEMD combined with wavelet threshold is generally higher than that of single EEMD, and the SNR of improved threshold is the highest when EEMD is combined with three threshold functions respectively. Therefore, the combination of EEMD and improved wavelet threshold is better. Then the energy entropy is extracted and input into SVM for classification

4.3 Analysis of SVM classification results.

In this paper, the training model is offline and the signal classification is online, so the time problem is not considered. Single vibration and sound signals are input into IFPA-SVM classifier respectively, and the classification accuracy is shown in Table 3. Faults 1, 2 and 3 respectively represent that the base is loose, refused to close, and the connecting rod of closing spring and opening spring falls off.

Table 3. Classification results of sound and vibration signals

Category	Normal	Fault 1	Fault 2	Fault 3	Average
Sound signal	80% (8/10)	100% (10/10)	90% (9/10)	40% (4/10)	77.5% (31/40)
Vibration signal	100% (10/10)	20% (2/10)	100% (10/10)	100% (10/10)	80% (32/40)

When IFPA-SVM classifier is used to diagnose single acoustic signal, the accuracy of fault 1 is 100%. When single vibration signal is used for diagnosis, the diagnostic accuracy of normal state, fault 2 and 3 is 100%. Based on this result, the classification accuracy can be improved by using the method of combination of sound and vibration. Then, the feature vectors of sound, vibration and acoustic vibration fusion are input into PSO-SVM, SFLA-SVM, FPA-SVM and IFPA-SVM respectively for comparison. The diagnosis results are shown in Table 4.

Table 4. Recognition accuracy of four classifiers

Classifier	Sound signal	Vibration signal	Acoustic vibration combined signal
PSO-SVM	65%	70%	77. 5%
SFLA-SVM	77. 5%	77. 5%	90%
FPA-SVM	77. 5%	77. 5%	90%
IFPA-SVM	77. 5%	80%	95%

ISSN: 2414-1895 DOI: 10.6919/ICJE.202104_7(4).0015

From the combination of sound and vibration signals, the accuracy of ifpa-svm classifier is higher than the other three classifiers, reaching 95%, which shows that IFPA algorithm can jump out of local optimum and find global optimal parameters. Compared with the single sound and vibration signal, the accuracy of the four classifiers is improved in different degrees. Therefore, the method of the combination of sound and vibration can effectively improve the accuracy of classification and recognition.

5. Summary

In this paper, the preprocessing method of EEMD and improved wavelet threshold is used to improve the low reconstruction accuracy of traditional single denoising method. The improved FPA algorithm is used to optimize the SVM classifier, which makes the algorithm jump out of the local optimum and get the global optimal value, which improves the accuracy of the classification model. Compared with the single signal method, the combined acoustic vibration method can reflect the fault state more comprehensively and effectively improve the accuracy of fault identification of circuit breaker, which has practical value in engineering.

In this paper, the sample size is small and can be expanded for training. In this paper, acoustic and vibration signals are used for feature extraction, and other characteristics such as current and force can be added to further describe fault features.

References

[1] Jiajin Qi, Xu Gao, Nantian Huang. Mechanical Fault Diagnosis of a High Voltage Circuit Breaker Based on High-Efficiency Time-Domain Feature Extraction with Entropy Features. Entropy. Vol. 22(2020), No. 4, p. 478.

[2] Linhuan Luo, Xiao Liu, Xiaohui Yan. Insulation fault identification of vacuum circuit breakers based on improved MFCC and SVM. Journal of Physics: Conference Series. Vol. 1176(2019), No. 6, p. 62027.

[3] Hengzhen Li, Yunfei Wang, J. F. Wang, et al. Support Vector Machine Based Fault Diagnosis Using Trip and Close Coil Current of Circuit Breakers. IEEE Region 10 Conference. Macao, PEOPLES R CHINA, 2015, p. 1-5.

[4] Yu Yao, Nan Wang. Fault diagnosis model of adaptive miniature circuit breaker based on fractal theory and probabilistic neural network. Mechanical Systems and Signal Processing. Vol. 142(2020), p. 106772.

[5] Shi Liu, Jin Tan, Fangang Meng, et al. Study of PSO-BP Neural Networks Application in High-Voltage Circuit Breakers Mechanical Fault Diagnosis. China International Conference on Electricity Distribution (CICED). Xian, PEOPLES R CHINA, 2016, pp. 1–5.

[6] Kang Sun, Yongchao Liu. Research on mechanical fault diagnosis of high voltage circuit breaker based on EEMD and mahalanobis distance discriminant. High Voltage Apparatus. Vol. 54(2018), No. 12, p. 43-49.

[7] Changpeng Su, Xuemei Wang, Zhe Xu, et al. Research on wavelet threshold de-noising method based on new threshold function. Tactical Missile Technology. Vol. 2020, No. 3, p. 66-72.

[8] Hao Fan, Xingwen Li, Haibo Su, et al. Research on circuit breaker fault diagnosis method based on principal component analysis-support vector machine optimization model. High Voltage Apparatus. Vol. 56(2020), No. 06, p. 143-151.

[9] Dawei He, Jingbo Peng, Jinhai Hu, et al. Bearing fault diagnosis based on a modified CS-SVM model optimized by an improved FOA algorithm. Journal of Vibration and Shock. Vol. 37(2018), No. 18, p. 108-114.

[10] Liuyu Huang, Shuping Gao, Junning Wang, et al. Hybrid frog leaping algorithm based on differential evolution. Systems Engineering and Electronics. Vol. 39(2017), No. 10, p. 2382-2392.

[11] Jiao Dai, Mingxin Zhang, Hao Sun, et al. Optimization of flower pollination algorithm. Computer Engineering and Design. Vol. 38(2017), No. 6, p. 1503-1509.

[12] X Yao, Y Liu, G Lin. Evolutionary Programming Made Faster. IEEE Transactions on Evolutionary Computation. Vol. 3(1999), No. 2, p. 82-102.